UPDATED APPLICATIONS OF ADVANCED COMPACT ACCELERATORS

M. Uesaka†, University of Tokyo, Tokyo, Japan

Abstract

We are working for downsizing of RF linacs from room-size to portable and table-top sizes and applying them to medical, industrial and social uses. Recently, we have proposed and designed a new S-band 35 MeV/35 kW linac γ-ray source for ^{99}Mo/^{99m}Tc (γ-emitter for medical diagnosis) production from ^{100}Mo target. Its construction will be finished within two years and the domestic production and even export will start then. The same system can be used for ^{225}Ac (α–emitter for cancer therapy) from ^{226}Ra target. We are proposing making the Mo/^{226}Ra target from nuclear wastes from nuclear power plants and fuel production plants. Next, we have developed portable 950 keV / 3.95 MeV X-band (9.3 GHz) electron linacs to on-site nondestructive inspection of industrial and social infrastructures such as chemical reaction chambers and bridges following the radiation safety law and regulation in Japan. By using the portable 950 keV / 3.95 MeV X-band electron linac based X-ray sources for on-site bridge inspection, we visualize inner reinforcement iron structure. The information of the iron states is used for the structural analysis of a bridge to evaluate its residual strength and sustainability. Table-top micro electron / ion beam sources using laser dielectric accelerating techniques are under development. The beam energy is ~ 1 MeV, the beam size is ~1 μm. We aim to apply them to 3D dynamic observation of radiation-induced DNA damage / repair for basic research of radiation therapy and low dose effect.

INTRODUCTION

We have been continuing developing and operating S-band linacs (35 / 18 MeV, room-size), X-band linacs (9.3 / 11.424 GHz , portable size) and laser accelerator dielectric accelerators (Yb laser of 1 mm, one-table-top size) at Nuclear Professional School, University of Tokyo for these 40 years as shown in Fig. 1.

This activity is really three-staged downsizing of RF linac.

S-BAND 35 MEV / 35 KW LINAC FOR MEDICAL RI PRODUCTION

Currently, the medical RI of ^{99}Mo/^{99m}Tc (γ-emitter for medical diagnosis) are produced by 6 research reactors in the world. Three out of the six are aged so that they are planned to be shut-downed within a few years. In Japan we are perfectly import them from the two countries. Since the two reactors are inspected at the same time, almost all supply was suspended last November. Thus, the supply is rather fragile so that we have to solve this problem by using accelerators. There are the two ways to use accelerators,

Figure 1: Three-staged downsizing of RF linac at University of Tokyo.

namely cyclotron and electron linac [1]. There must be advantages and drawbacks in the both ways. Then, our group has decided to choose the latter based on the advantage of the overall performance of the system. We have proposed and designed the optimized S-band 35 MeV/35 kW linac γ-ray source for domestic and stable production and supply. About five / fifty systems are estimated to meet the whole demands in Japan and the world, respectively. We have chosen 100 keV thermionic electron gun, buncher system two traveling-wave type acceleration tubes and the 5 MW / 770 Hz clystrons of CANNON E37307. The power of 35 kW is determined based on the consideration of beam loading. The system layout is depicted in Fig. 2. The left / right-hand sides correspond to the linac and Mo target irradiation areas, respectively.

† uesaka@tokai.t.u-tokyo.ac.jp

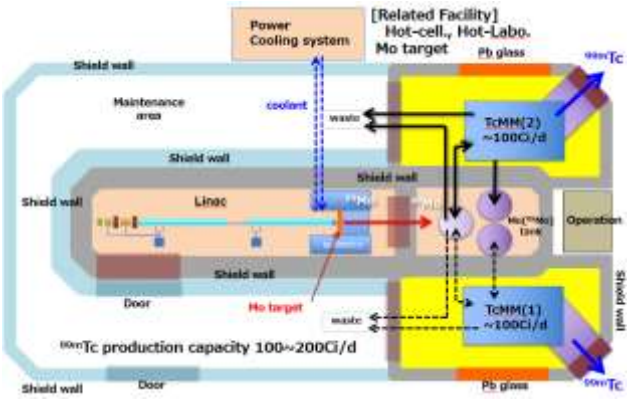

Figure 2: Layout of S-band 35 MeV / 35 kW linac and chemical processing devices for ^{99}Mo /^{99m}Tc.

Although the linac and chemical processing devices become home-made, solid targets of extremely high impurity ^{100}Mo and ^{226}Ra for ^{99}Mo/^{99m}Tc and ^{225}Ac are manufactured by using the centrifuge technique. Now we are proposing an alternative methodology to solve the above issue. We plan to use nuclear wastes from U fuel production and spent fuels in nuclear power generation. We chemically extract Mo of chemically extremely high purity from U mine wastes and ^{226}Ra of extremely high impurity from high level liquid nuclear waste as shown in Fig. 3. Then, we manufacture the solid targets after the extraction. We are collaborating on this process with Japan Atomic Energy Agency (JAEA).

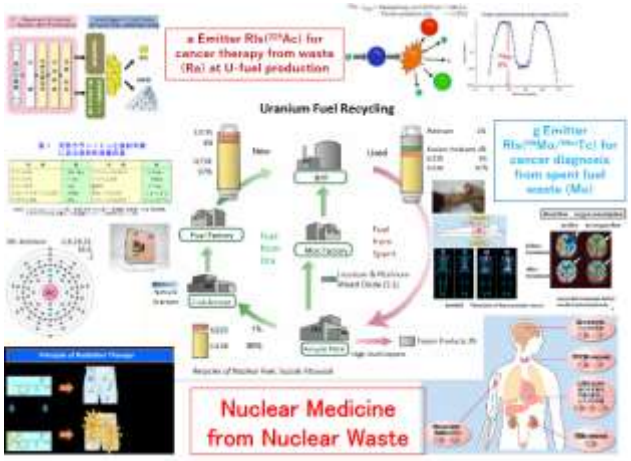

Figure 3: Scheme of ^{99}Mo /^{99m}Tc and ^{226}Ra production from nuclear wastes in Japan.

X-BAND PORTABLE LINACS FOR BRIDGE INSPECTION

We used X-band (9.3 GHz) linac based 950 keV / 3.95 MeV X-ray sources for the inspection of the actual bridge. The systems and their major parameters are given in Figs 4 and 5 and Tables 1 and 2, respectively [2].

We also adopted the side-coupled standing wave type accelerating structure. Electrons are injected into a Tungsten target that generates bremsstrahlung X-rays. The generated X-rays are collimated by a Tungsten collimator into the shape of a cone which has an opening angle of 17 degrees. Most important is the X-ray intensity, which is 50 mSv/min at 1 m for a full magnetron RF power of 250 kW. The system consists of a 50 kg X-ray head, 50 kg magnetron box, and stationary electric power source and water chiller unit. The X-ray head and magnetron box are portable, and because they are connected to each other by a flexible waveguide, only the position and angle of the X-ray head are finely tuned. We have optimized the design with respect to X-ray intensity, compactness, and weight. The parameters of the 950 keV X-ray source are summarized in the table of Fig. 4. We place an X-ray detector on the opposite site of the X-ray source between the object and source to detect the transmitted X-rays through the object. We use a flat panel detector (FPD) from Perkin Elmer Corporation for the detector.

The 3.95 MeV system is shown in Fig. 5. This system consists of a 62 kg X-ray head with target collimator of 80 kg, magnetron box of 62 kg, electric power sources of 116 kg, and water cooling system of 30 kg. The X-ray head and magnetron box are portable and the position and angle of the former are also finely tuned. The X-ray intensity of this system is 2 Gy/min at 1 m.

Calculated attenuations in concrete for the X-rays from the 950 keV / 3.95 MeV sources are shown in Fig. 6. The results indicate that concrete with thicknesses of up to 400 mm and 800 mm can be penetrated by the 950 keV / 3.95 MeV sources, respectively.

We comply with Japan's Law Concerning Prevention of Radiation Hazards Due to Radioisotopes and Regulations on Prevention of Ionizing Radiation Hazards when we use the 950 keV / 3.95 MeV X-ray sources in the field for on-site bridge inspection. According to law, an electron beam source below 1 MeV is not an accelerator. Thus, we comply with this regulation. The 950 keV X-ray source is registered with the local agency of labor supervision. We usually operate the source in a radiation controlled area which has a radiation safety system complying with the Regulations on Prevention of Ionizing Radiation Hazards. Use of the source outside the controlled area is also allowed. In this case, we temporally set up a controlled area at the measurement site, and place sufficient shielding around the source and object to suppress the air dose rate below 1.3 mSv / 3 months. Moreover, we have to set a temporal facility boundary of 250 μSv / 3 months Amendment of the law that allows use of accelerators below 4 MeV only for on-site bridge inspection was implemented in Japan in 2005. After we completed governmental registration as a radiation source, we submitted for permission of use outside the radiation controlled area. Finally, we performed the on-site inspection under the Regulations on Prevention of Ionizing Radiation Hazards similar to the 950 keV case.

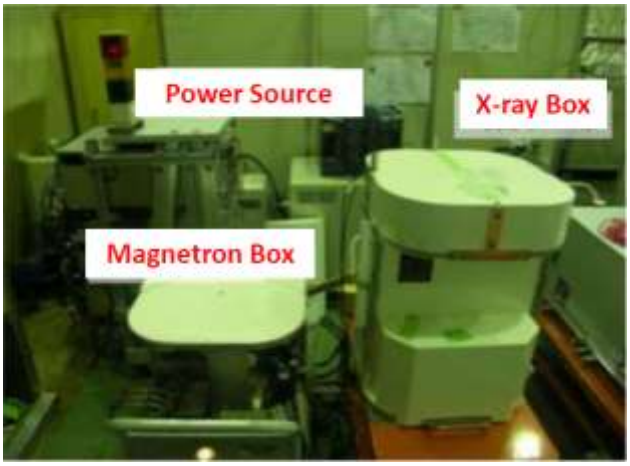

Figure 4: 950 keV portable X-band linac based X-ray source. The maximum X-ray energy is 950 keV. The system consists of three units: X-ray head, magnetron, and power units.

Table 1: Major parameters of 950 keV portable X-band linac based X-ray source

Operating frequency	9300 MHz
Beam energy	950 keV
Beam current	130 mA
Pulse width	2.5 μs
Pulse frequency	330 pulses/s
RF power	250 kW
Electron gun voltage	20 kV
Accelerator length	125 mm
Q-value of the accelerator	7150
X-ray size at target	0.7 mm
X-ray intensity at 1 m	> 50 mGy/min

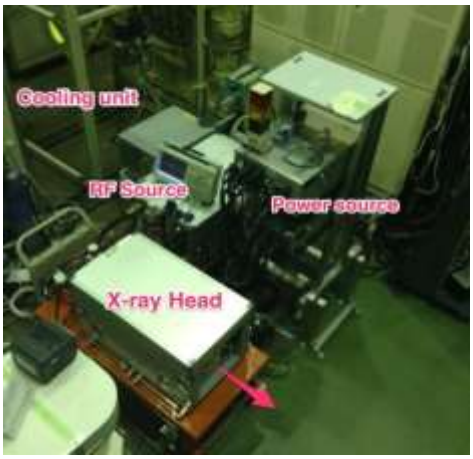

Figure 5: 3.95 MeV portable X-band linac based X-ray source. The system consists of four units: X-ray head, magnetron, power, and chiller units.

Table 2: Major parameters of 3.95 MeV portable X-band linac based X-ray source

Main Unit	Accelerating Tube	RF Source	HVPS Control
Weight [kg]	80+62 (Collimator+ Accelerating tube)	62	116
Parameters	Electron gun output current 300 mA	Frequency 9.3 GHz	
	Electron gun voltage 20 kV	Pulse width 4 μs	
	Beam current 100 mA	Repetition rate 200 pps	
		RF power output 1.5 MW	

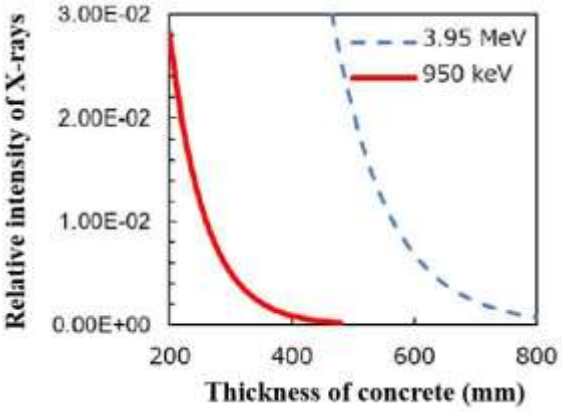

Figure 6: Calculated results of attenuation for the X-rays in concrete from the 950 keV / 3.95 MeV X-ray sources.

An X-ray flat panel detector (FPD) and imaging plate (IP) are used for X-ray imaging acquisition. By using the FPD, on-line measurement in seconds is available so that sparse and fine tuning of the position of the X-ray sources and detector can be accomplished. Stacking measurement in minutes is more appropriate for the IP. Imaging processing of IPs can be carried out on-site immediately. An aerial work platform and stage are used for measurement of bridges. The X-ray source can be installed inside a box for bottom floor slab inspection or on a pedestal for upper slabs of box-shaped bar types with help of a crane.

Figure 7 shows typical transmission images of the inner structure of the slab of a certain T-shaped bar type bridge obtained by the 950 keV X-ray source. We successfully observed the inner structure in detail with the linac based X-ray system. The PC wires were clearly visualized. Cutting and thinning of PC wires are clearly apparent. Reduction of the PC wire cross sections are estimated

visually and images are used for the structural analysis to evaluate any reduction of structural strength quantitatively.

PC wires, sheath, and grout in a web part of other T-shaped bar types obtained by the 950 keV X-ray source are given in Fig. 8. Even grout filling and missing grout are clearly visible.

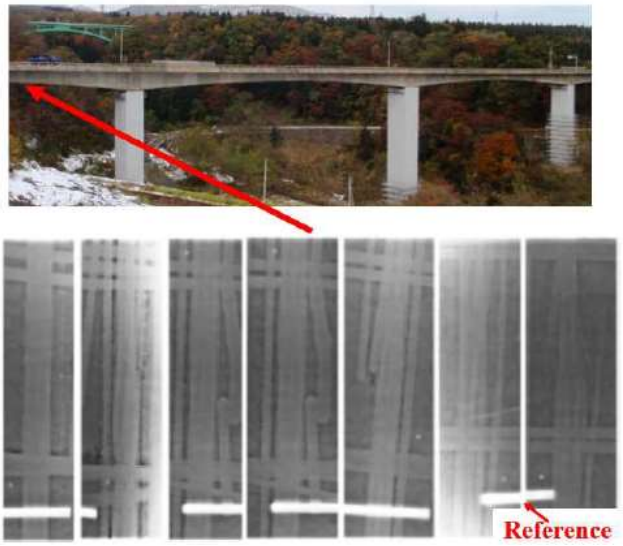

Figure 7: Series of X-ray images of PC wires in a bottom slab of a box-shaped bar type bridge acquired by the 950 keV X-ray source. Cutting and thinning of PC wires are observed.

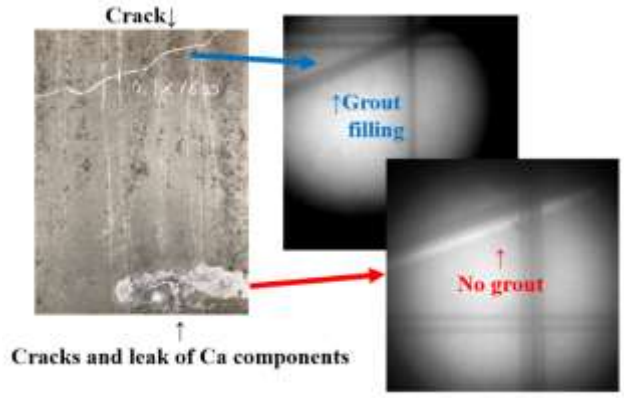

Figure 8: Surface view and X-ray transmission images of near PC wires, sheath, and grout in a web part of a T-shaped bar type bridge acquired by the 950 keV X-ray source. Cracks and leak of Ca components are visible. Moreover, grout filling and missing grout are clearly observed in the near PC sheath.

Public Works Research Institute of Japan and the University of Tokyo are developing new technical guidelines for special inspections of bridges using 950 keV / 3.95 MeV X-ray sources. An overview is provided in Fig. 9. First, visual and hammer sound inspection screening should be performed based on regular inspection guidelines. Advanced hardware and software techniques such as drawn and acoustic analysis are adopted in this step. If degraded parts are found, the special X-ray transmission inspection is performed using the 950 keV or 3.95 MeV X-ray sources, depending on the thickness of the concrete containing the degraded parts. Here, the states of PC wires and rods as affected by corrosion, cuts, and reduction of cross sections are quantitatively evaluated with spatial resolution of 1 mm. Then, 3D nonlinear structural analysis is performed to evaluate the degradation of the structural strength quantitatively. Based on this evaluation, repair, reinforcement, or other decisions should be reviewed. Several inspection industries are joining our project and technical transfer is being promoted. We hope to soon apply these guidelines to all aged bridges in Japan and finally across the world.

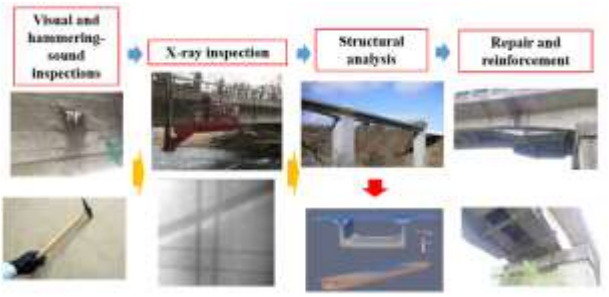

Figure 9: Guidelines for special X-ray transmission inspection using 950 keV / 3.95 MeV X-ray sources accompanied with visual and hammering-sound inspections, structural analysis, final repair, and/or reinforcement.

LASER DIELECTRIC ACCELERATOR FOR RADIATION BIOLOGY

Electron LDA system for radiation biology as shown in Fig. 10 is under development [3]. We plan to use 200 keV thermionic electron gun and accelerate electrons up to 1 MeV. The beam size is about 1 $\mu m\phi$ and is focused on to DNA in a nucleus of cell. Dynamic microscopic observation of DNA damage and repair can be done by using a time-lapse microscopy. DNA repair is visualized by using a repairing protein such as GFP-XRCC1.

We are doing a basic design of LDA system. We plan to use two laser pulses and inject them to a pair of LDA gratings made by SiO_2 in order to form a symmetric accelerating field between a pair of gratings (see Fig. 11). We are running CST code for 2D electromagnetic field calculation and electron acceleration. We design 121 types of gratings in order to match the longitudinal phase velocity to the velocity of electrons at each grating. The period of pitch of grating becomes longer for lower energy. Typical electric field intensity profile, time variation of longitudinal electric field and energy gain as a function of longitudinal coordinate around 900 keV are given in Fig. 12.

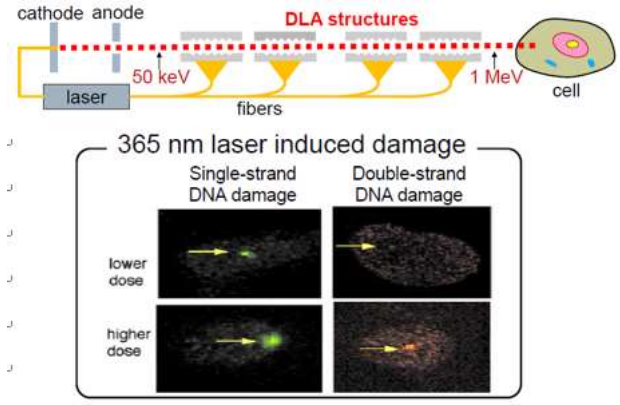

Figure 10: Laser dielectric accelerator for radiation biology. Dynamic observation of damage and repair of DNA is available. The examples using micro-spot UV laser are shown at the left bottom.

Time variation of the longitudinal electric field indicates that the field contains both accelerating π-mode and non-accelerating 0-mode. Thus, periodic acceleration and deceleration by the 0-mode rides on monotonous energy increase by the π-mode. There is a maximum accelerated energy for each grating as given in Fig. 13. The Maximum energies at the initial energies of 200 and 900 keV for different injection phases. Therefore, we set the number of pitches up to the maximum energy. The ratio of the o-mode to the π-mode increases and the longitudinal electric field also decease as the matched phase velocity decrease. This is one of difficulties of LDA. Electron energy as a function of the longitudinal coordinate is shown in Fig. 14. Although the energy gain in lower energy is small, regular LDA is achieved for more than ~600 keV. Bunching performance is depicted in Fig. 15. Finally, ~100 attosecond bunch is formed in this case. We are also manufacturing a SiO_2 grating as depicted in Fig. 16.

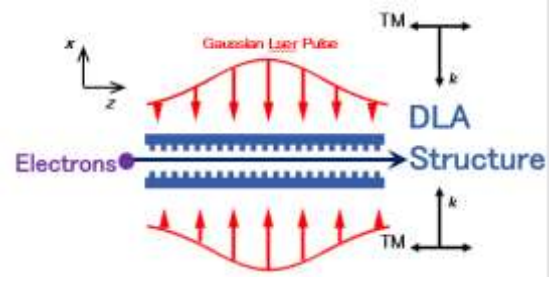

Figure 11: Two laser pulse scheme with a set of gratings.

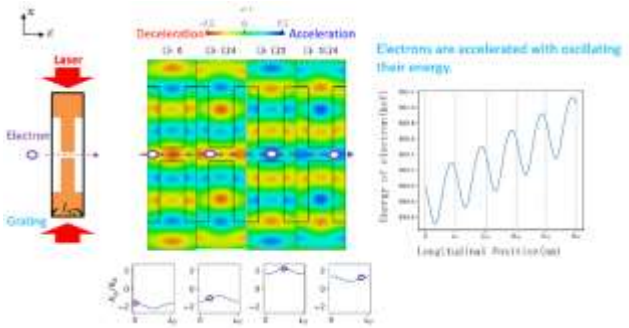

Figure 12: Calculated electric field intensity (upper middle), time-variation of longitudinal electric field (lower middle) and energy gain as a function of longitudinal coordinate around 900 keV.

Finally, the image of one-table-top LDA system is drawn in Fig. 17. We are going to replace UV laser with the LDA system. The analysing system can be used as it is now.

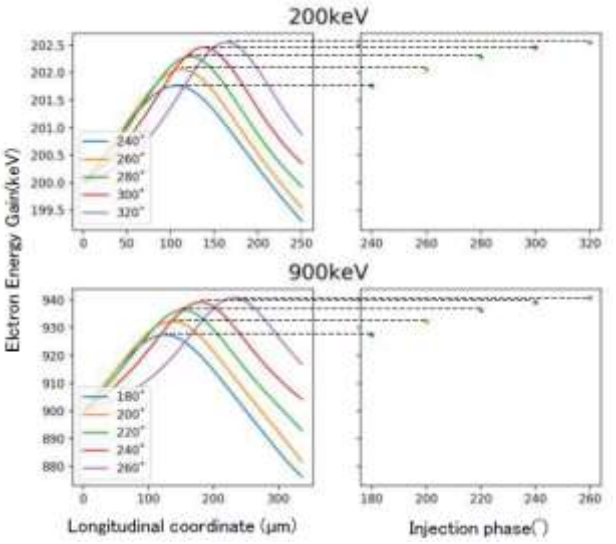

Figure 13: Maximum energies of the two gratings at the initial energies of 200 and 900 keV for different timings of injection.

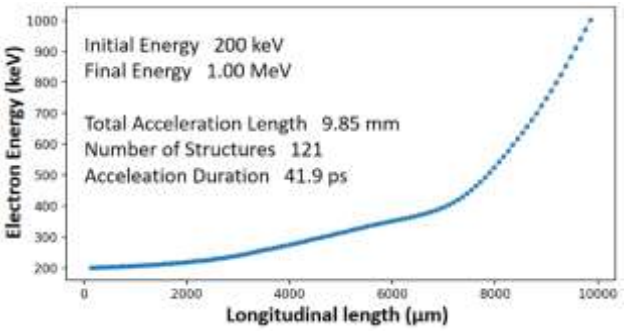

Figure 14: Calculated electron acceleration from 200 keV to 1 MeV by 121 gratings.

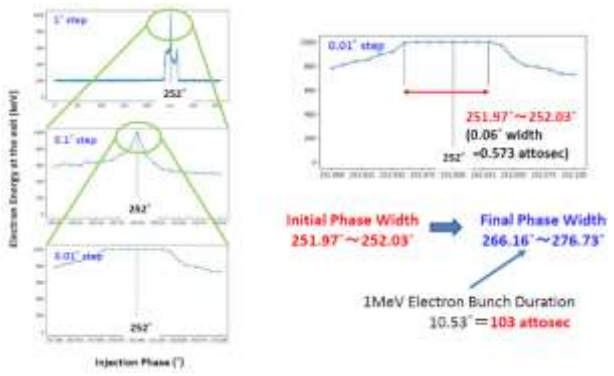

Figure 15: Bunching performance. 100 attosecond bunch is formed.

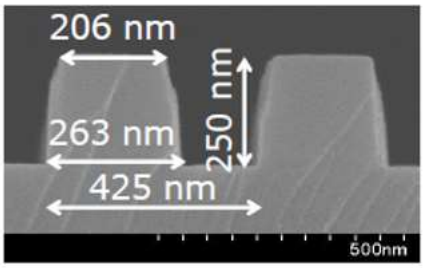

Figure 16: Manufactured grating structure.

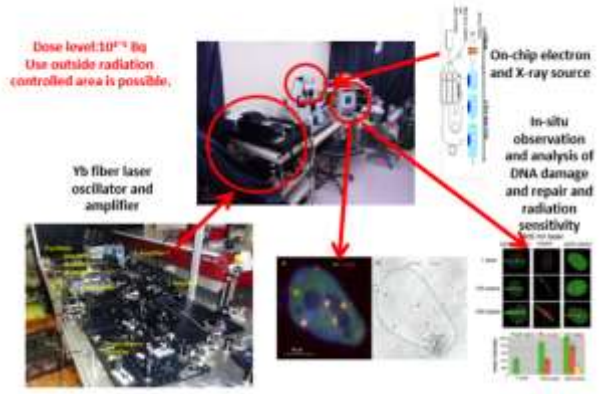

Figure 17: Image of one-table-top micro beam LDA system for radiation biology.

ACKNOWLEDGEMENTS

We would like to deeply thank to the collaboration of Accuthera Inc.,Public Works Research Institute, National Accelerator Development Laboratory (KEK) and Tohoku University.

REFERENCES

[1] J. Jang and M. Uesaka, "Influence of enriched ^{100}Mo on Mo reaction yields", *J. Phy.s Commu.*, vol. 3, no. 5, p. 055015, May 2019. doi:10.1088/2399-6528/ab1d6b

[2] M. Uesaka *et al.*, "On-site Bridge Inspection by 950 keV / 3.95 MeV Portable X-band Linac X-ray Sources", *Bridge Optimization - Inspection and Condition Monitoring*, IntechOpen, 2018. doi: 10.5772/ intechopen. 82275

[3] Z. Chen, K. Koyama, M. Uesaka, M. Yoshida, and R. Zhang, "Resonant enhancement of accelerating gradient with silicon dual-grating structure for dielectric laser acceleration of subrelativistic electrons", *Appl. phys. Let.*, vol. 112, p. 034102, 2018.